

Original Article

Molecular mechanisms involved in TGF- β 1-induced Muscle-derived stem cells differentiation to smooth muscle cells

Xiang Tang, Xianghui Su, Zhuohui Zhong, Canliang Wen, Tiansong Zhang, Yali Zhu

Department of Gynecology, Guangzhou Women and Children's Medical Center, Guangzhou Medical University, Guangzhou 510623, China

Received March 6, 2019; Accepted July 30, 2019; Epub August 15, 2019; Published August 30, 2019

Abstract: We investigated the molecular mechanisms involved in transforming growth factor beta 1 (TGF- β 1)-induced myogenic stem cell differentiation to smooth muscle cells. We isolated muscle-derived stem cells (MDSCs) from gastrocnemius muscles following their identification by immunohistochemistry analysis of desmin and flow cytometry analysis of SCA-1, CD34, and CD45. MDSCs at passage 3 (PP3) were cultured *in vitro* to examine the effects of MDSC induction. Gene ontology and KEGG pathway analyses were performed to analyze these differentially expressed genes. Reduced representation bisulfite sequencing was performed in TGF- β 1-treated and untreated cells to evaluate differences in the methylation status and analyze the chromosomal distribution of differentially methylated sites (DMSs). Significant morphological changes to cells were observed at PP3, and most PP3 cells were positive for desmin and SCA-1, and were confirmed to be MDSCs. Results of western blot and immunohistochemistry analyses suggested that expressions of α -SMA and CNN1 significantly increased after treatment with TGF- β 1. Global transcriptome analysis identified 1996 differentially expressed genes (MSC_TGF β 1/MSC_NC). Results of methylome analysis indicated that there were more hypermethylation sites in the untreated group than in the TGF- β 1-treated group. Most DMSs were hypermethylated, whereas a small portion was hypomethylated. The chromosomal distribution of DMSs indicated that chromosome 1 had the highest proportion of DMSs, whereas the Y chromosome had the fewest DMSs. *Sud2*, *Pcdh19*, and *Nat14* are potential core genes involved in cell differentiation. These results may explain the mechanisms of cell differentiation and provide useful information regarding diseases such as pelvic organ prolapse.

Keywords: Pelvic organ prolapse, TGF- β 1, muscle-derived stem cells, transcriptome, methylome

Introduction

Pelvic organ prolapse (POP) is a pelvic floor disorder that often occurs in women with pelvic floor support defects. A previous study reported that implantation of non-absorbable polypropylene mesh in the vagina is an effective method for treating this disease [1]. However, clinical trials found that adverse reactions, such as mesh exposure and complications caused by rejection [2], are common, with an incidence of 10%-30% [3]. Methods to increase the thickness of the vaginal mucosa and reduce complications are required to resolve this. Currently, there is the use of stem cells that are implanted on synthetic material and induced into smooth muscle cells has become an impor-

tant research topic [4-6]. Muscle-derived stem cells (MDSCs) are adult stem cells, which possess multidifferentiation potential, isolated from skeletal muscle. In the human body, skeletal muscle is rich and easy to obtain; therefore, an increasing number of researchers have focused on this cell type [7]. A previous study induced differentiation of MDSCs in smooth muscle cells to treat urinary incontinence [8].

Transforming growth factor beta (TGF- β) is a ubiquitous multifunctional regulator in humans and has been shown to regulate cell growth, differentiation, and injury repair [9]. It acts predominantly via the TGF- β -Smad signaling pathway to exert its biological functions [10]. Smad proteins are important signal transduction and

Molecular mechanism of TGF- β 1-induced differentiation

are regulatory molecules for the TGF- β superfamily. Phosphorylation of Smads stimulated via activated receptors could combine with Smad4 forming protein complex, which conducts signals from the cell membrane into the nucleus to regulate the transcription of target genes, resulting in various biological effects [10]. TGF- β is located in the regulation center of smooth muscle cell differentiation, as observed in *in vitro* culture. It has been shown to inhibit proliferation of human aortic endothelial cells (HAECs) and may also act to convert HAECs into mesenchymal cells. Therefore, TGF- β plays an important role in maintaining smooth muscle cell differentiation and inducing other cells types to differentiate into smooth muscle cells [11]. Epigenetics is a gene expression regulation mechanism that changes the phenotype without changing the primary structure of the DNA, and includes DNA methylation, histone modification, chromosome remodeling, and RNA interference. DNA methylation is one of the most important epigenetic modifications and is widespread in most eukaryotes. CpG dinucleotide formation is the main type of methylation that occurs in the human genome and has attracted recent attention. Gene activity has been shown to be associated with CpG island methylation (known as imprinted genes), X-chromosome inactivation, cell aging, and tumors [12]. Epigenetic abnormalities that provide an alternative mechanism of transcriptional silencing are highly activated in cancers. Methylation of CpG islands in tumor suppressor genes prevents RNA polymerase from binding and initiating transcription.

The present study investigated the molecular mechanisms involved in TGF- β 1-induced myogenic stem cell differentiation into smooth muscle cell. We isolated MDSCs from gastrocnemius muscle and cultured the isolated cells *in vitro*, followed by induction with 10 ng/mL TGF- β 1 for 10 days. Immunohistochemistry and western blot analysis of α -SMA (actin) and CNN1 (calponin) expression were performed. We analyzed the transcriptome and compared differentially expressed and methylated genes, and constructed an interaction network.

Method and materials

MDSC isolation and identification

The present study was approved by The Institute Research Medical Ethics Committee

of Guangzhou medical University. Three-week-old Sprague-Dawley rats were purchased from Forevergen Biosciences (Forevergen, Guangzhou, China). The rats were sterilized using 75% alcohol. Gastrocnemius muscles without fat, tendon, nerves, and blood vessels were isolated and rinsed with phosphate-buffered saline (PBS). The detailed operational procedures were performed exactly as previously reported [13]. Cultured cells were washed with cold PBS (Gibco, USA) then fixed with 100% methanol at -20°C for 15 min, and blocked with blocking solution (1% bovine serum albumin diluted in PBS) for 30 min at room temperature. Cells were then incubated with anti-desmin (Sigma-Aldrich) primary antibody (diluted 1:500 in blocking solution) at 4°C for 4 h. Cells were then incubated with anti-mouse secondary antibody (Vector Laboratories, Burlingame, CA, USA) at room temperature for 1 h. An LSM 510 META confocal microscope was used to capture images (Zeiss, Oberkochen, Germany). For flow cytometry analysis, cells were digested in 0.1% trypsin-EDTA (Gibco, USA). Cells were then centrifuged at 1000 rpm for 5 min at 4°C and collected according to cell passage number (PP1, PP2, PP3, PP4, PP5, and PP6). Residual medium and trypsin were removed using PBS and cells were counted under the microscope. Cells were transferred to 1.5 mL EP tubes and resuspended in 200-300 μ L PBS, and a cell ratio of 1 μ g/10⁶ was used to add the flow antibodies (SCA1, CD34, and CD45). The treated cells were incubated at 4°C for 30 min. Excess antibody was washed using 1 mL of PBS. The cells were then resuspended in 500 μ L of PBS and stored on ice prior to flow cytometry analysis.

MDSC differentiation and identification

Medium from PP3 MDSCs was removed, and the cells were washed with PBS. This procedure was repeated three times. Induction buffer comprising high-glucose Dulbecco's modified Eagle medium (Gibco, USA), 10% fetal bovine serum (Sigma-Aldrich, USA), 10% horse serum (Gibco, USA), 0.5% chick embryo extract (Life Technology, USA), 100 U/mL double antibody (Gibco, USA), and 10 ng/mL TGF- β 1 (Acris Antibodies, Herford, Germany) [14] was added to the PBS-washed PP3 MDSCs. The culture medium was changed every two days, and subculture was performed every three to four days. Ten days after induction, differentiated cells were identified by immunofluorescence and

Molecular mechanism of TGF- β 1-induced differentiation

western blot analyses. For immunofluorescence analysis, 1×10^3 /mL induced MDSCs were collected and seeded onto 6-well plates. After two days, the culture medium was removed, and cells were washed three times with cold PBS. The treated cells were immediately fixed with 4% paraformaldehyde (Sigma-Aldrich, USA) for 30 min at room temperature. Subsequently, 0.5% TritonX-100-PBS was added and incubated for 30 min after washing three times with PBS. Next, 10% goat serum (Gibco, USA) was used to block for 30 min, then mouse anti- α -SMA (1:100), anti-CNN1 (1:100), and anti-GADH (1:100) were added to the cells and incubated overnight at 4°C. Cy3-conjugated goat anti-mouse was added dropwise into pretreated cells and incubated for 2 h at 37°C. The cells were washed with PBS then viewed under a fluorescence microscope. For western blot analysis, the cells were washed twice with PBS and transferred to a serum-free medium. After 72 h, the supernatants were collected in 1.5 mL EP tubes. Protein samples (20 mg) were resolved using sodium dodecyl sulfate-polyacrylamide gel electrophoresis (6% acrylamide gel) then electroblotted onto PVDF membranes. The membranes were incubated with an anti-Coll II antibody (1:500 dilution; Gibco, USA). Signal development was detected using an ECL kit (Solarbio life sciences). Densitometry was measured using ImageJ (ImageJ, USA).

Transcriptome

RNA was extracted from 1×10^6 cells treated with or without TGF- β 1 for 10 days using the PicoPure RNA isolation kit (Arcturus Engineering, USA). RNase-free DNase was added in a one-column treatment step (Qiagen, USA). Total RNA was quantified using a NanoDrop ND-1000 spectrophotometer (Thermo Fisher, USA). RNA integrity was assessed by gel electrophoresis using an Experion bioanalyzer (BioRad, USA) then stored at -80°C. Purified RNA was reverse transcribed using the SMARTer PCR cDNA Synthesis Kit (Clontech, USA). cDNA libraries were prepared using 2.0 μ g of amplified cDNA. Samples were then fragmented, indexed, and sequenced using Illumina HiSeq2500 at Forevergen (Forevergen, China) in GuangZhou. One hundred bases of paired-end reads were applied in this study. The human genome (hg19) was used as the reference genome. To obtain unique sequence reads, we

applied the following criteria: (1) minimum length fraction ≥ 0.9 ; (2) minimum similarity fraction ≥ 0.8 ; and (3) maximum number of two mismatches. The reads per kilobase per million mapped reads (RPKM = total exon reads/mapped reads in millions \times exon length in kb) method was used to normalize the data [15]. We employed a false discovery rate (FDR ≤ 0.001) and \log_2 Ratio ≥ 1 to screen for differentially expressed genes between the two groups (with or without 10-day induction treatment) [16]. Heat maps were created using software package in R with default settings. Gene ontology (GO) and KEGG pathway analyses were performed using DAVID according to the default actions.

Methylome analysis

DNA was extracted from 1×10^6 cells from the two groups (with or without 10-day induction treatments) using QIAamp DNA Mini Kit (Qiagen, USA). Next, 100 U of MspI (NEB, USA) was added to 5 μ g of genomic DNA to digest for 16 h at 37°C. MspI was then inactivated by heating to 80°C for 20 min. The Illumina Paired-End library preparation strategy was followed to construct sequencing libraries, which contained End Repair, "A" base addition, and methylated-adaptor ligation. The library was evaluated using 2% TAE agarose gel. Bands at 155-225 and 225-335 base pairs (bps) were excised. The MiniElute PCR Purification Kit (QIAGEN, USA) was used to recover the DNA using columns with 20 μ L elution buffer. Bisulfite was used added to the EZ DNA Methylation-Gold kit (ZYMO, USA) and bisulfite-treated products were amplified using a 50- μ L PCR reaction system, which contained 10 μ L of treated DNA, 1 μ L of 10 mM dNTPs, 1 μ L of PCR primer A, 1 μ L of PCR primer B, 5 μ L of 10 \times master mix buffer, 0.5 μ L of JumpStart TaqDNA polymerase, and 31.5 μ L of water. PCR was performed as follows: 94°C for 1 min; 11 cycles of 94°C for 30 s, 58°C for 30 s, and 72°C for 30 s; and 72°C for 5 min. PCR products were purified and recovered using QIAamp DNA Mini Kit (Qiagen, USA), followed by sequencing using Illumina HiSeq2500 at Forevergen (Forevergen, China) in GuangZhou. Next, 49-bp reads without adaptor sequences were mapped to the human reference genome (hg19). Two rounds of alignment were conducted in parallel with the strand specificity of DNA methylation. BGI

SOAPaligner version 2.01 was used to identify the strand specificity of DNA methylation [17], which allows up to two mismatches for successful mapping. Surrogate variable analysis was used to identify CpG loci that showed significant differences in DNA methylation between the treated and untreated groups [18]. An FDR correction was applied at the 0.05 level for multiple testing. Paired *t* test was used to assess the significance of DNA methylation differences between two groups. $P < 0.01$ was considered significant for differential DNA methylation between the two groups.

Quantitative real-time PCR (qRT-PCR)

Total RNA in the cells were isolated using TRIzol (Invitrogen, USA) and then reverse transcribed into first strand cDNA using a M-MLV reverse transcriptase kit (Promega,) according to the manufacturer's protocol. Next, the qRT-PCR was performed using ChamQ SYBR qPCR Master Mix (Vazyme,) using cDNA as the template. GAPDH was used as an internal standard. The following thermocycling conditions were used: 95°C for 120 s, 40 cycles of 95°C for 15 s, and then 60°C for 30 s. The primer sequences were as follows: RAT-Susd2: 5'-CCTCCTTGTCCTCCGTCCTAGA-3' (sense) and 5'-GAGCTCTCAAGTTGGGCCAT-3' (antisense), RAT-Nat14: 5'-AGTTACCCGCCTCTCTGTCT-3' (sense) and 5'-AGCCACAGGCCTCCAATAAC-3' (antisense), RAT-Pcdh19: 5'-CCGGGACTGTGATCGCTAAT-3' (sense) and 5'-CACAGCAGGTCTCGGTC-AAT-3' (antisense).

Statistical analysis

SPSS 19.0 software (IBM, USA) was used to perform the statistical analyses. The mean values of the statistical results for the measured data were presented as the mean \pm standard error. Statistical differences among groups were analysed by one-way analysis of variance (ANOVA). And the differences between the two groups were calculated using Tukey's test. *P*-values less than 0.05 were defined as significantly different.

Results

MDSC isolation and identification

Morphological changes of isolated MDSC were previously observed at different time points

[13]. The improved differential adhesion method isolates cells according to cell well adhesion speed. Separated cells were divided into different stages according to the well adhesion time: (1) PP1, 0 h; (2) PP2, 2 h; PP3, 2 days; PP4, 3 days; PP5, 4 days; and PP6, 5 days. It was possible to isolate MDSCs (PP6) due to their slow adhesion well speed compared with other type cells. PP1 and PP2 cells were predominantly fibroblasts, which possess significant features such as fusiform shape, abundant presence, fast growth, and short well adhesion time. Significant morphological changes were observed from PP3. Most PP3-PP5 cells were identified as vascular endothelial and smooth muscle cells, which were low in number and showed low well adhesion. We employed immunohistochemistry methods to evaluate the desmin status in PP1 and PP3 cells (**Figure 1A**). The results indicated that rare desmin-positive MDSCs were detected in PP1. Most PP1 cells were identified as fibroblasts by morphology. However, desmin-positive cells were confirmed as MDSCs in most PP3 cells. We also performed flow cytometry analysis on PP3 cells. Three FITC-labeled antibodies, including SCA-1, CD34, and CD45, were used to identify MDSCs in PP3 cells (**Figure 1B**). A total of 77.4% of the PP3 cells were SCA-1-positive, showing strong evidence for MDSCs; however, 4.5% were CD34-negative, and 5.4% were CD45-positive, which was lower than expected and could have been due to the primary isolation method. In summary, we confirmed that the majority of PP3 cells were MDSCs.

MDSC differentiation and identification

To examine the effects of inducing differentiation, we used immunohistochemistry and western blot analyses to identify differentiated cells 10 days after induction using 10 ng/mL TGF- β 1. Immunohistochemistry analysis indicated that α -SMA and CNN1 expression was significantly higher in the treated group compared with the untreated group. Fluorescent microscopy revealed that the distribution of α -SMA and CNN1 in myogenic stem cells was fascicular, which concurred with the characteristic distribution of α -SMA along microtubules (**Figure 2A** and **2B**). The cell morphology in the untreated and treated groups gradually changed from a slender spindle shape and became round or polygonal. Meanwhile, high α -SMA and CNN1

Molecular mechanism of TGF- β 1-induced differentiation

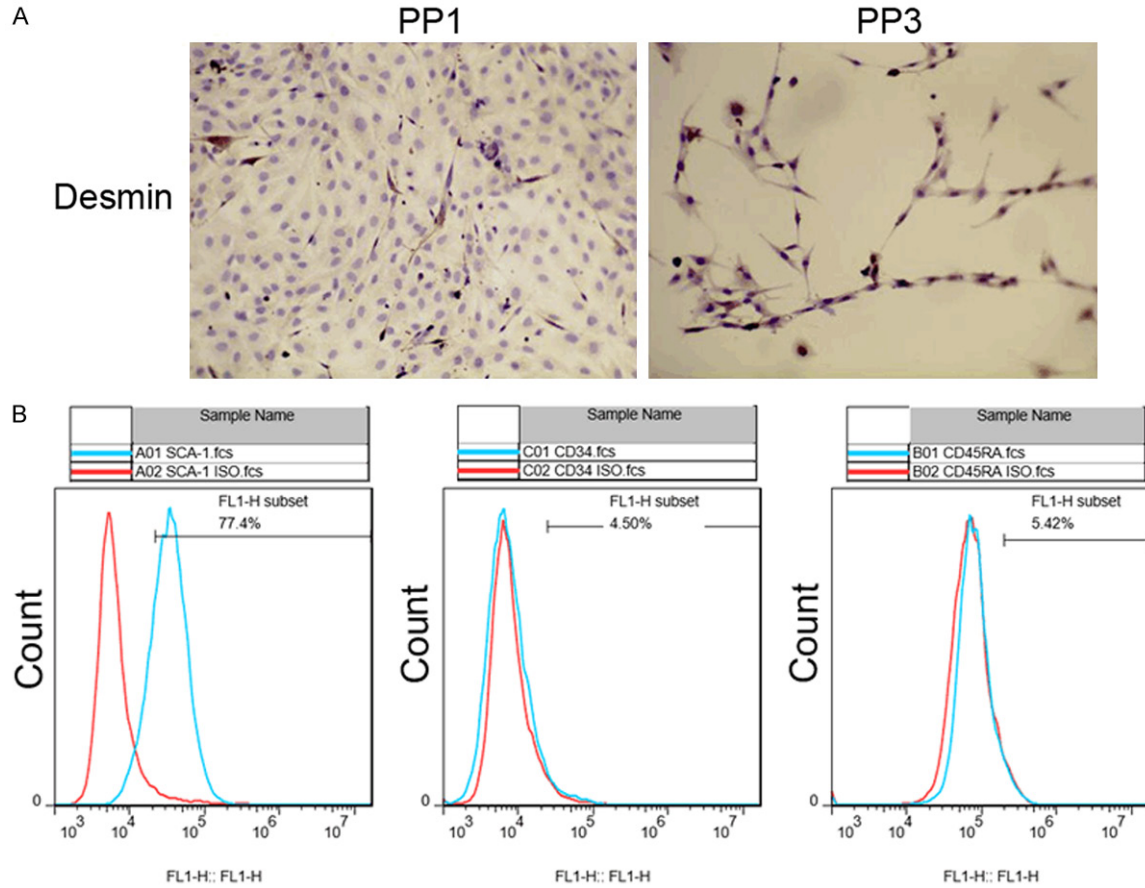


Figure 1. MDSC were identified by immunohistochemistry and flow cytometry analysis. MDSC were isolated from rat gastrocnemius muscles. A. Immunohistochemistry analysis of desmin status in PP1 and PP3 cells. B. Flow cytometry analysis of SCA-1, CD34, and CD45 in PP3 cells. MDSC: Muscle Derived Stem Cells.

expression in the TGF- β 1-treated group was confirmed by western blot analysis. These findings suggested that the primary isolated MDSCs successfully differentiated into smooth muscle cells.

Transcriptome analysis

To assess the transcript abundance in the untreated and TGF- β 1-treated groups, we performed next-generation sequencing for global transcriptome analysis. An average of 26,942,821 read pairs were harvested per sample. Expression levels for each gene and differential expression analysis was then determined. For gene expression analysis, we detected mRNA expression for 12,410 genes in the untreated group and 12,666 genes in the TGF- β 1-treated group (Table S1 and Figure 3A). We then compared the two datasets to identify differentially expressed genes and

found that 1996 genes were differentially expressed (MSC_TGF β 1/MSC_NC) (Table S2 and Figure 3B). Of these 1996 genes, 837 were significantly upregulated in the MSC_TGF β 1 group compared the MSC_NC group, including Car3 ($P = 0.00$; FDR = 0.00), Afap1l2 ($P < 0.001$; FDR < 0.001), and Dcdc2 ($P \leq 0.001$; FDR < 0.001). We found that 1159 genes were significantly upregulated in the MSC_TGF β 1 group compared with the MSC_NC group, such as Nos2 ($P < 0.001$; FDR < 0.001), Scin ($P < 0.001$; FDR < 0.001), and Mmp13 ($P < 0.001$; FDR < 0.001). We further analyzed the chromosomal distribution of the 1996 differentially expressed genes (Figure 3C). The results suggested that these differentially expressed genes were located on all rat chromosomes except the Y chromosome, which may be due to two main reasons: (1) the length of the Y chromosome is smaller than other chromosomes, and genes involved in TGF- β 1-related pathways

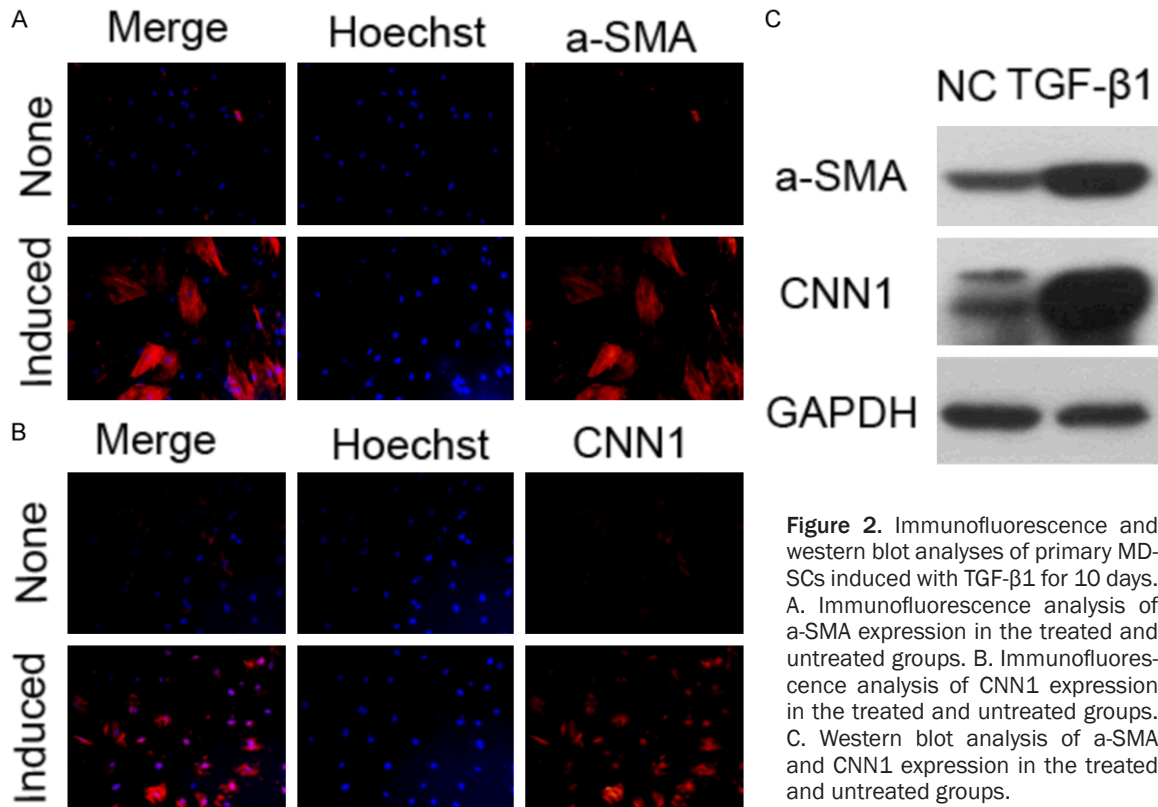


Figure 2. Immunofluorescence and western blot analyses of primary MD-SCs induced with TGF-β1 for 10 days. A. Immunofluorescence analysis of a-SMA expression in the treated and untreated groups. B. Immunofluorescence analysis of CNN1 expression in the treated and untreated groups. C. Western blot analysis of a-SMA and CNN1 expression in the treated and untreated groups.

were not located on this chromosome; or (2) genes involved in TGF-β1 related pathways were located on the Y chromosome. However, experimental errors, sequencing errors, and/or strict screening criteria applied in this study meant that we were unable to determine this. It was also noted that more genes were downregulated than upregulated on chromosomes 1, 2, 3, 4, 5, 7, 8, 9, 10, 11, 13, 14, 15, 16, 18, 19, and 20. On contrary, there were more upregulated genes on chromosomes 12, 17, and X compared with the number of downregulated genes. We performed GO and KEGG pathway analyses of these differentially expressed genes. GO analysis identified biological processes, cellular components, and molecular functions (Figure S1 and Table S3). For biological processes, cellular process (GO: 0009987, corrected P -value = $5.40E-141$), metabolic process (GO: 0008152, corrected P -value = $8.56E-97$), and pigmentation (GO: 0043473, corrected P -value = 0.02) were the top three significantly enriched terms. For cellular components, cell (GO: 0005623, corrected P -value = $3.3E-116$), and cell part (GO: 0044464, corrected P -value = $1.82E-114$) were the top two significantly enriched terms. From molecular function, binding (GO: 0005488, corrected P -

value = $2.16E-140$) was the most significantly over-represented term. KEGG is a database resource for understanding high-level functions and utilities of the biological system (<http://www.genome.jp/kegg/>). In the present study, the differentially expressed genes were involved in 283 pathways (Figure S2 and Table S4). It was noted that 146 pathways showed corrected P -values <0.01 . Figure S2 and Table S4 show the results of the pathway enrichment, which clearly shows that metabolic pathways were the highest enriched term. Furthermore, 156 differentially expressed genes identified in our study participated in this pathway. It is worth noting that pathways in cancer, PI3K-Akt signaling pathway, focal adhesion, and cytokine-cytokine receptor interaction were also significantly enriched in this study.

Methylome analysis

We performed reduced representation bisulfite sequencing in the two groups to evaluate differences in methylation status. We harvested an average of 42,151,229 read pairs from the TGF-β1-treated and untreated groups. Figure 4A shows the chromosomal distribution of the methylation sites. The results indicated that

Molecular mechanism of TGF- β 1-induced differentiation

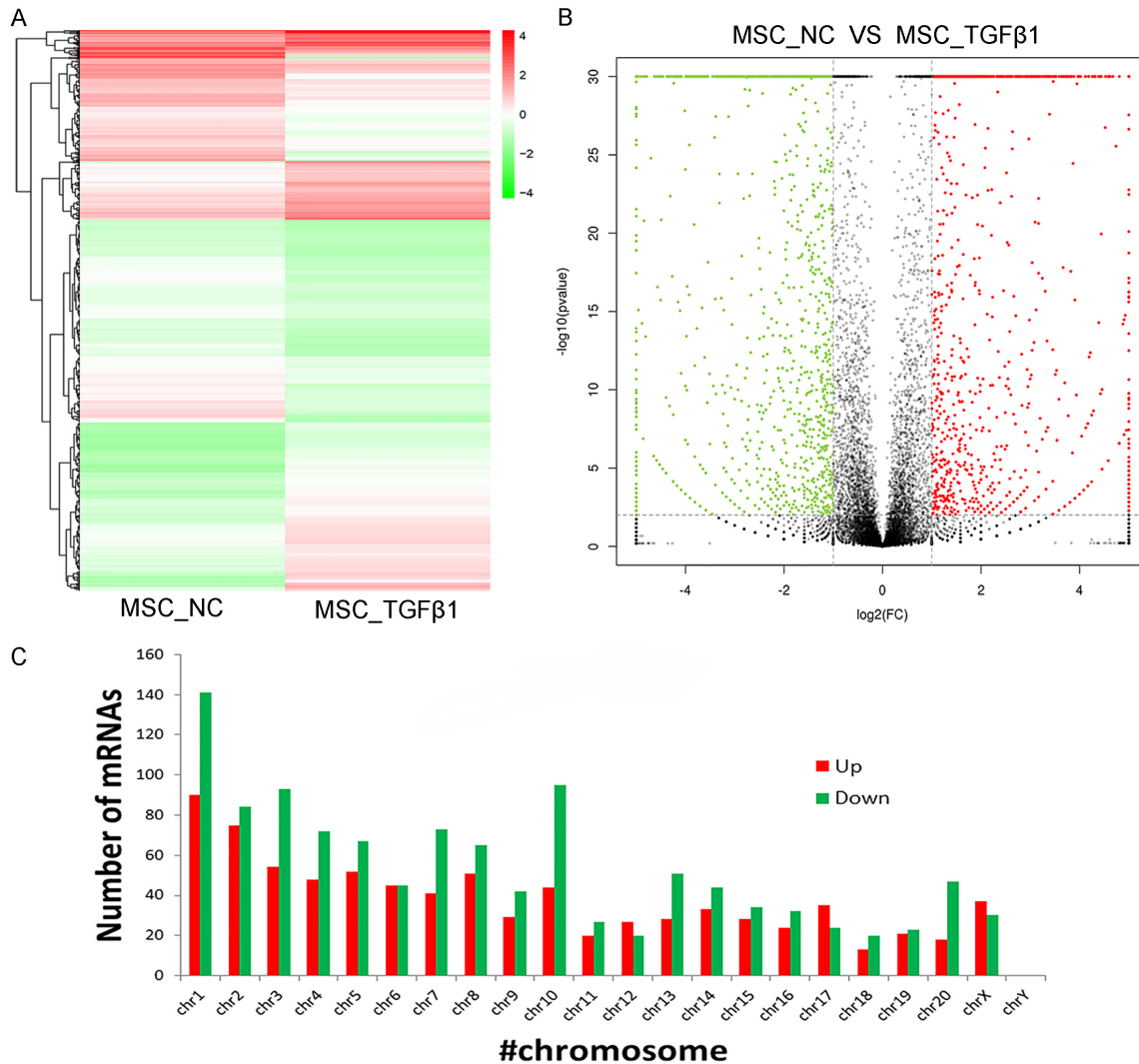


Figure 3. Transcriptome data analysis of the TGF- β 1-treated and untreated groups. A. Heat map analysis of transcript abundance in the treated and untreated groups. B. Volcano plot analysis of differentially expressed genes in the treated and untreated groups. C. Chromosomal distribution of the differentially expressed genes.

there were more methylation sites in the untreated group compared with the TGF- β 1-treated group in each chromosome, suggesting lower gene expression in the untreated group than in the TGF- β 1-treated group. Furthermore, these methylated sites were distributed among different genetic components, including gene body, upstream, downstream, exon, intron, CDS, 5' UTR, and 3' UTR (Figure 4B and 4D). In both groups, most of the methylated sites were located in gene bodies, and exon and intron regions. We compared the distribution of differentially methylated sites (DMSs) in TGF- β 1 treated and untreated groups. Figure 4C shows that the majority of DMSs were hypermethylated, whereas a small portion was hypomethylated, indicating that hypermethylation is

the main form of epigenetic modification. These hypermethylated sites represent an effective way to inhibit gene expressions. The chromosomal distribution of DMSs indicated that chromosome 1 possessed the most DMSs, whereas the Y chromosome had the fewest. We speculated that this result may have been due to differences in chromosomal length.

Overlap of the transcriptome and methylome

We compared the two datasets to identify overlap of differentially expressed and methylated genes. The results indicated that three genes, including *Sud2*, *Pcdh19*, *Nat14*, were downregulated in the TGF- β 1-treated group compared with the untreated group. Furthermore, these genes were hypermethylated in the TGF- β 1-

Molecular mechanism of TGF-β1-induced differentiation

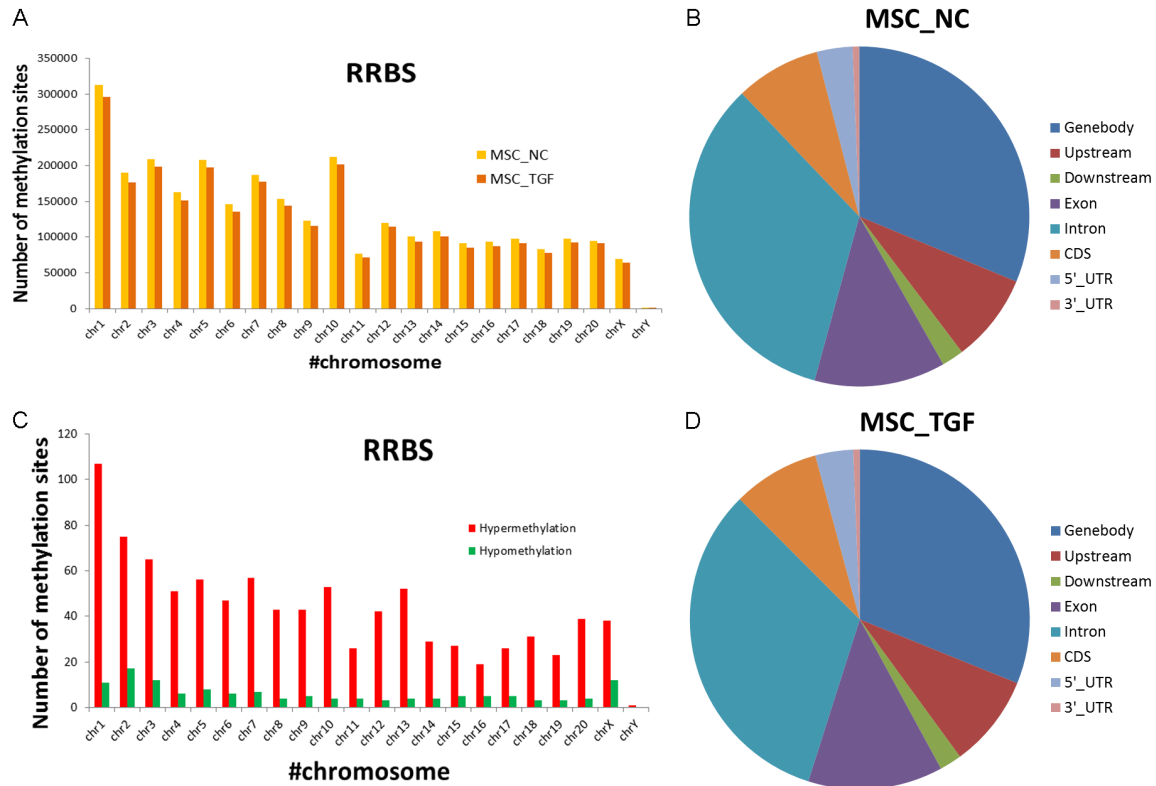


Figure 4. Methyome data analysis the TGF-β1-treated and untreated groups. A. Chromosomal distribution of the methylation sites in the treated and untreated groups. B. Distribution of the methylated sites in the untreated group. C. Chromosomal distribution of the differentially methylated sites. D. Methylated site distribution in the TGF-β1-treated group.

treated group compared with the untreated group. These results were consistent with a previous study that reported that hypermethylation of genes would inhibit their expression [19]. **Figure 5** shows the interaction networks for Sud2, Pcdh19, and Nat14. Pcdh19 directly interacted with eight genes, including Pkp1, Ctnd1, Pkp2, Ctnd2, Jup, Pkp3, Pkp4, and Arvcf. Armadillo-like proteins are characterized by a series of armadillo repeats, and were first defined as a *Drosophila* “armadillo” gene product. Members of the p120 (ctn)/plakophilin subfamily of armadillo-like proteins include CTNND1, CTNND2, PKP1, PKP2, PKP4, and ARVCF. PKP4 may be a component of desmosomal plaque and other adhesion plaques, and is thought to be involved in regulating junctional plaque organization and cadherin function [20]. Sud2 may directly interact with all six genes, and is reported to be related to a tumor suppressor and susceptibility gene for amyotrophic lateral sclerosis (ALS). Finally, Nat14 could only interact with NAT3. To further validate the next-

generation sequencing results, we designed mRNA primers to amplify the three downregulated genes (Sud2, Pcdh19, Nat14). qRT-PCR results showed that Sud2, Pcdh19, Nat14 were down-regulated in the TGF-β1-treated group compared with the untreated group, which were consistent with the sequencing results (**Figure 6**).

Discussion

There are currently two main methods to induce differentiation of MDSCs in smooth muscle cells: (1) the smooth muscle coculture method; and (2) the growth factor induction method. While the smooth muscle coculture method has been applied in various studies [21-23], it is difficult to isolate specific cell types using this method. In the present study, we used TGF-β1 as growth factor inducer to convert MDSC into smooth muscle cells. TGF-β1 is a multifunctional growth factor that can promote stem cell proliferation. It may also be used to induce differentiation of mesenchymal

Molecular mechanism of TGF-β1-induced differentiation

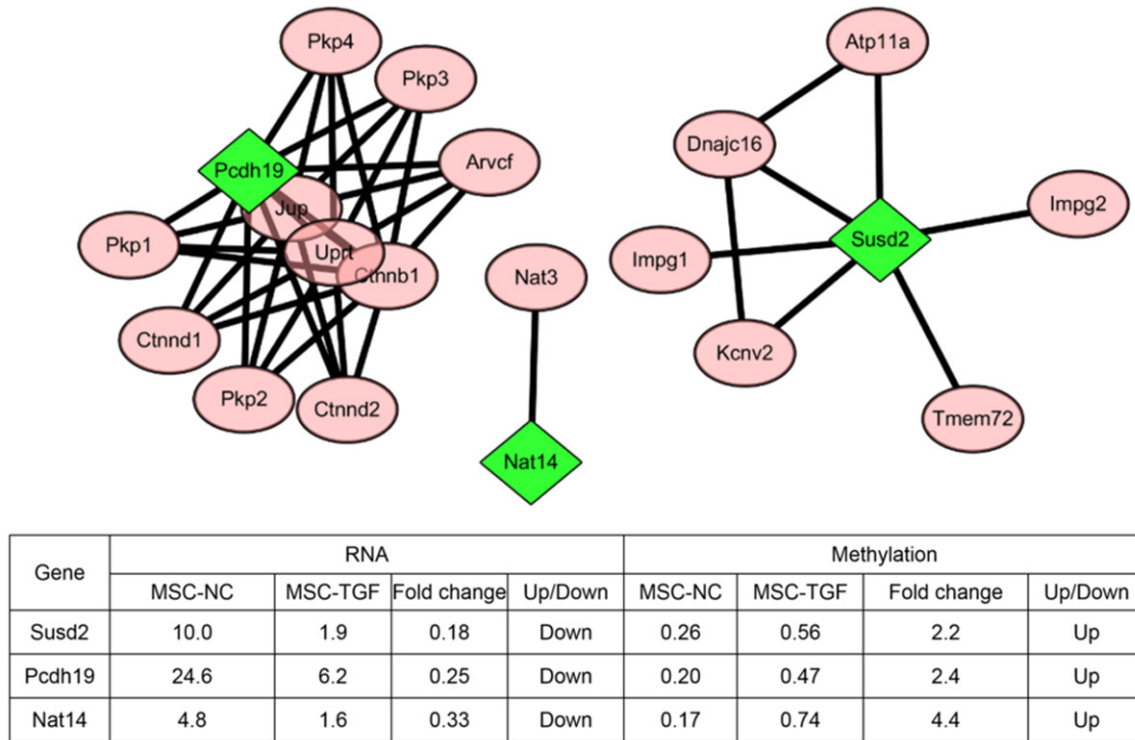


Figure 5. Interaction networks of SUSD2, Pcdh19, and Nat14 genes. Interactions between the three genes were extracted by searching the STRING database with a confidence cutoff value of 0.900 (<https://string-db.org/>). The interaction network was reconstructed by using the Cytoscape software. Green diamonds indicate genes with higher methylation and lower mRNA abundance in the TGF-β1-treated group compared with the untreated group.

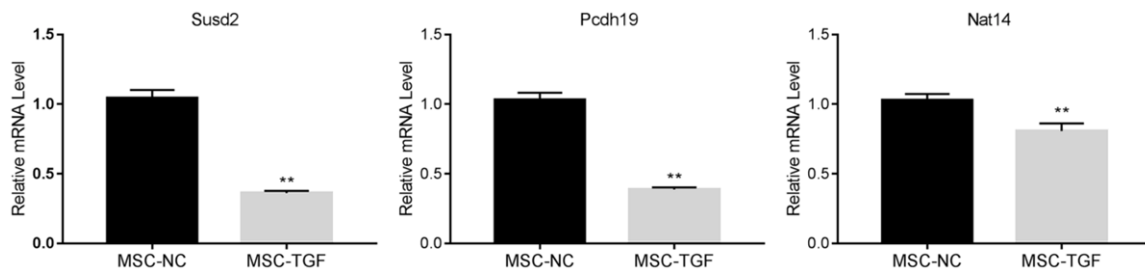


Figure 6. The gene expression of SUSD2, Pcdh19, and Nat14 were detected by qRT-PCR in the TGF-β1-treated group and the untreated group. **P<0.01.

stem cells in smooth muscle [11]. Actin (α -SMA) is a highly conserved protein that is expressed in all eukaryotic cells. It plays important roles in cell movement and maintenance of cell morphology, and is widely distributed in almost all smooth muscle cells [24]. Meanwhile, calponin (CNN1) is a smooth muscle-specific regulatory protein. It is abundantly expressed in differentiated smooth muscle cells and is involved in actin cytoskeletal remodeling by binding to the cytoskeletal protein actin. Calponin has been widely reported to be a smooth muscle contrac-

tion regulator [25-27]. A previous study suggested that treatment with 0.1-10 ng/mL TGF-β1 inhibits mesenchymal stem cell proliferation. As a smooth muscle growth marker, expression of calponin (CNN1) is increased in response to increasing concentrations of TGF-β1. This suggests that TGF-β1 not only initiates differentiation to smooth muscle but also promotes the differentiation rate [28]. In the present study, treatment with 10 ng/mL TGF-β1 could induce myogenic stem cell differentiation. While induced MDSCs showed a slow

Molecular mechanism of TGF- β 1-induced differentiation

growth rate, expression of α -SMA and CNN1 significantly increased, which was similar to the findings of a previous study [28]. Moreover, the distribution of smooth muscle actin in myogenic stem cells was fascicular after 10 days of treatment, which was consistent with the characteristic distribution of α -SMA along microtubules [29].

Epigenetic abnormalities provide an alternative mechanism of transcriptional silencing. Methylation of CpG islands in tumor suppressor genes prevents RNA polymerase from binding and initiating transcription [30]. In the present study, we focused on the genes that showed downregulated mRNA expression and upregulated methylation levels in TGF- β 1-induced cells compared with that in untreated cells. Three genes, *SUSD2*, *Pcdh19*, and *Nat14*, were identified and confirmed by qRT-PCR. Protocadherin 19 (*PCDH19*) encodes a protein belonging to the δ -cadherin superfamily, which is highly expressed in brain. Members of this family play important roles in vertebrate nerve conservation during evolution [31]. *PCDH19* is the pathogenic gene of epilepsy and mental retardation limited to females (EFMR). The relationship between *PCDH19* and EFMR was first reported by Dibbens et al. [32]. Liu et al. [33] reported that *PDCH19* was mainly expressed in the dorsal and lateral sides of the central nervous system as well as the spinal cord in brain tissue in zebrafish. Meanwhile, *PDCH19* was also detected in developing eyeballs, the retina, and ear buds, and was also expressed in the developing hippocampus and amygdala of humans and rats [34]. A previous study suggested that mutations or deletions in the *PDCH19* gene lead to calcium-dependent intercellular adhesion dysfunction [32]. Yagi et al. speculated that this may be related to its role in the signal transduction of synaptic membrane and connection between neurons [35]. However, the detailed biological role of *PDCH19* remains unclear. The *SUSD2* gene is mainly expressed in brain, kidney, and lung [36]. Previous studies have identified its roles as a novel tumor suppressor and susceptibility gene for ALS [36, 37]. Mutations in the *SUSD2* gene could affect the von Willebrand factor type D domain, and induce apoptosis in HeLa cells [36]. *SUSD2* has been shown to induce apoptosis via caspase-3 and caspase-9, similar to TP53 [38]. Therefore, it is speculated that *SUSD2* may be involved in the apoptosis of neu-

rons in ALS [37]. *NAT14* (*KLP1*) was identified in 2001 [39]. *Klp1* cDNA comprises 1346 bps and contains an open reading frame of 206 amino acids [40]. *KLP1* belongs to the kinesin superfamily proteins (KIFs), which have been shown to transport organelles, protein complexes, and mRNA to specific destinations in a microtubule and ATP-dependent manner [41]. KIFs are not only involved in the transport of organelles, protein complexes, and mRNAs but also participate in chromosomal and spindle movements during mitosis and meiosis [42, 43]. However, evidence for the biological functions of *KLP1* is poor.

Conclusion

In the present study, we successfully isolated MDSCs from gastrocnemius muscle using a previously reported improved method. MDSCs were cultured in vitro and induced by treating with 10 ng/mL TGF- β 1 for 10 days. Protein expression analysis of α -SMA and CNN1 indicated successful induction. Moreover, mRNA abundance analysis in the TGF- β 1-treated and untreated groups indicated that 1996 genes were differentially expressed (*MSC_TGF β 1/ MSC_NC*). These differentially expressed genes were subjected to GO and KEGG pathway analyses. Single-organism process (GO: 0044699, corrected *P*-value <0.01) was the top enrichment item of GO analysis. Pathways in cancer (*rno05200*, corrected *P*-value <0.01) was the top enrichment item in the KEGG analysis. Methylome analysis revealed that there were more hypermethylation sites in the untreated group compared with the TGF- β 1-treated group. The majority of DMSs were hypermethylated, whereas a small portion was hypomethylated, indicating that hypermethylation was the main form of epigenetic modification. The chromosomal distribution of DMSs indicated that chromosome 1 possessed the most DMSs, whereas the Y chromosome had the fewest. We also compared the differentially expressed and methylated genes. *Sud2*, *Pcdh19*, and *Nat14* were identified as potential core genes involved in cell differentiation. These results may contribute to a better understanding of the process of cell differentiation, and may help in the treatment of diseases such as POP.

Acknowledgements

This research was supported by the Guangdong Natural Science foundation (2015A030-

310105), and the Guangzhou medical and health science and technology project (20161A-011070).

Disclosure of conflict of interest

None.

Address correspondence to: Dr. Yali Zhu, Department of Gynecology, Guangzhou Women and Children's Medical Center, Guangzhou Medical University, No. 9 Jinsui Road, Tianhe District, Guangzhou 510623, China. Tel: 020-38076114; Fax: 020-380-76114; E-mail: 21558034@qq.com

References

[1] Jia X, Glazener C, Mowatt G, MacLennan G, Bain C, Fraser C and Burr J. Efficacy and safety of using mesh or grafts in surgery for anterior and/or posterior vaginal wall prolapse: systematic review and meta-analysis. *BJOG* 2008; 115: 1350-1361.

[2] Zhu L, Lang J, Sun Z, Ren C, Liu X and Li B. Pelvic reconstruction with mesh for advanced pelvic organ prolapse: a new economic surgical method. *Menopause* 2011; 18: 328-332.

[3] Abed H, Rahn DD, Lowenstein L, Balk EM, Clemons JL and Rogers RG; Systematic Review Group of the Society of Gynecologic Surgeons. Incidence and management of graft erosion, wound granulation, and dyspareunia following vaginal prolapse repair with graft materials: a systematic review. *Int Urogynecol J* 2011; 22: 789-798.

[4] Takanari K, Hashizume R, Hong Y, Amoroso NJ, Yoshizumi T, Gharaibeh B, Yoshida O, Nonaka K, Sato H, Huard J and Wagner WR. Skeletal muscle derived stem cells microintegrated into a biodegradable elastomer for reconstruction of the abdominal wall. *Biomaterials* 2017; 113: 31-41.

[5] Collado MS, Cole BK, Figler RA, Lawson M, Manka D, Simmers MB, Hoang S, Serrano F, Blackman BR, Sinha S and Wamhoff BR. Exposure of induced pluripotent stem cell-derived vascular endothelial and smooth muscle cells in coculture to hemodynamics induces primary vascular cell-like phenotypes. *Stem Cells Transl Med* 2017; 6: 1673-1683.

[6] Murphy WL, McDevitt TC and Engler AJ. Materials as stem cell regulators. *Nat Mater* 2014; 13: 547-557.

[7] Stangel-Wojcikiewicz K, Majka M, Basta A, Stec M, Pabian W, Piwowar M and Chancellor MB. Adult stem cells therapy for urine incontinence in women. *Ginekol Pol* 2010; 81: 378-381.

[8] Mitterberger M, Marksteiner R, Margreiter E, Pinggera GM, Frauscher F, Ulmer H, Fussenegger M, Bartsch G and Strasser H. Myoblast and fibroblast therapy for post-prostatectomy urinary incontinence: 1-year followup of 63 patients. *J Urol* 2008; 179: 226-231.

[9] Sakaki-Yumoto M, Katsuno Y and Derynck R. TGF-beta family signaling in stem cells. *Biochim Biophys Acta* 2013; 1830: 2280-2296.

[10] Zi Z, Chapnick DA and Liu X. Dynamics of TGF-beta/Smad signaling. *FEBS Lett* 2012; 586: 1921-1928.

[11] Coll-Bonfill N, Musri MM, Ivo V, Barbera JA and Tura-Ceide O. Transdifferentiation of endothelial cells to smooth muscle cells play an important role in vascular remodelling. *Am J Stem Cells* 2015; 4: 13-21.

[12] Li E and Zhang Y. DNA methylation in mammals. *Cold Spring Harb Perspect Biol* 2014; 6: a019133.

[13] Gharaibeh B, Lu A, Tebbets J, Zheng B, Feduska J, Crisan M, Peault B, Cummins J and Huard J. Isolation of a slowly adhering cell fraction containing stem cells from murine skeletal muscle by the preplate technique. *Nat Protoc* 2008; 3: 1501-1509.

[14] Xu Z, Shen MX, Ma DZ, Wang LY and Zha XL. TGF-beta1-promoted epithelial-to-mesenchymal transformation and cell adhesion contribute to TGF-beta1-enhanced cell migration in SMMC-7721 cells. *Cell Res* 2003; 13: 343-350.

[15] Mortazavi A, Williams BA, McCue K, Schaeffer L and Wold B. Mapping and quantifying mammalian transcriptomes by RNA-Seq. *Nat Methods* 2008; 5: 621-628.

[16] Audic S and Claverie JM. The significance of digital gene expression profiles. *Genome Res* 1997; 7: 986-995.

[17] Li R, Yu C, Li Y, Lam TW, Yiu SM, Kristiansen K and Wang J. SOAP2: an improved ultrafast tool for short read alignment. *Bioinformatics* 2009; 25: 1966-1967.

[18] Leek JT and Storey JD. Capturing heterogeneity in gene expression studies by surrogate variable analysis. *PLoS Genet* 2007; 3: 1724-1735.

[19] Moore LD, Le T and Fan G. DNA methylation and its basic function. *Neuropsychopharmacology* 2013; 38: 23-38.

[20] Keil R, Schulz J and Hatzfeld M. p0071/PKP4, a multifunctional protein coordinating cell adhesion with cytoskeletal organization. *Biol Chem* 2013; 394: 1005-1017.

[21] Wallace CS and Truskey GA. Direct-contact coculture between smooth muscle and endothelial cells inhibits TNF-alpha-mediated endothelial cell activation. *Am J Physiol Heart Circ Physiol* 2010; 299: H338-346.

[22] McBane JE, Cai K, Labow RS and Santerre JP. Co-culturing monocytes with smooth muscle cells improves cell distribution within a degradable polyurethane scaffold and reduces in-

Molecular mechanism of TGF- β 1-induced differentiation

- flammatory cytokines. *Acta Biomater* 2012; 8: 488-501.
- [23] Dorweiler B, Torzewski M, Dahm M, Ochsenhirt V, Lehr HA, Lackner KJ and Vahl CF. A novel in vitro model for the study of plaque development in atherosclerosis. *Thromb Haemost* 2006; 95: 182-189.
- [24] Tokita Y, Akiho H, Nakamura K, Ihara E and Yamamoto M. Contraction of gut smooth muscle cells assessed by fluorescence imaging. *J Pharmacol Sci* 2015; 127: 344-351.
- [25] Winder SJ and Walsh MP. Calponin: thin filament-linked regulation of smooth muscle contraction. *Cell Signal* 1993; 5: 677-686.
- [26] Gao H, Steffen MC and Ramos KS. Osteopontin regulates alpha-smooth muscle actin and calponin in vascular smooth muscle cells. *Cell Biol Int* 2012; 36: 155-161.
- [27] Liu R and Jin JP. Calponin isoforms CNN1, CNN2 and CNN3: regulators for actin cytoskeleton functions in smooth muscle and non-muscle cells. *Gene* 2016; 585: 143-153.
- [28] Gong Z and Niklason LE. Small-diameter human vessel wall engineered from bone marrow-derived mesenchymal stem cells (hMSCs). *FASEB J* 2008; 22: 1635-1648.
- [29] Kamata H, Tsukasaki Y, Sakai T, Ikebe R, Wang J, Jeffers A, Boren J, Owens S, Suzuki T, Higashihara M, Idell S, Tucker TA and Ikebe M. KIF5A transports collagen vesicles of myofibroblasts during pleural fibrosis. *Sci Rep* 2017; 7: 4556.
- [30] Sproul D and Meehan RR. Genomic insights into cancer-associated aberrant CpG island hypermethylation. *Brief Funct Genomics* 2013; 12: 174-190.
- [31] Hulpiau P and van Roy F. Molecular evolution of the cadherin superfamily. *Int J Biochem Cell Biol* 2009; 41: 349-369.
- [32] Dibbens LM, Tarpey PS, Hynes K, Bayly MA, Scheffer IE, Smith R, Bomar J, Sutton E, Vandeleur L, Shoubridge C, Edkins S, Turner SJ, Stevens C, O'Meara S, Tofts C, Barthorpe S, Buck G, Cole J, Halliday K, Jones D, Lee R, Madison M, Mironenko T, Varian J, West S, Widaa S, Wray P, Teague J, Dicks E, Butler A, Menzies A, Jenkinson A, Shepherd R, Gusella JF, Afawi Z, Mazarib A, Neufeld MY, Kivity S, Lev D, Lerman-Sagie T, Korczyn AD, Derry CP, Sutherland GR, Friend K, Shaw M, Corbett M, Kim HG, Geschwind DH, Thomas P, Haan E, Ryan S, McKee S, Berkovic SF, Futreal PA, Stratton MR, Mulley JC and Gecz J. X-linked protocadherin 19 mutations cause female-limited epilepsy and cognitive impairment. *Nat Genet* 2008; 40: 776-781.
- [33] Liu Q, Chen Y, Kubota F, Pan JJ and Murakami T. Expression of protocadherin-19 in the nervous system of the embryonic zebrafish. *Int J Dev Biol* 2010; 54: 905-911.
- [34] Kim SY, Mo JW, Han S, Choi SY, Han SB, Moon BH, Rhyu IJ, Sun W and Kim H. The expression of non-clustered protocadherins in adult rat hippocampal formation and the connecting brain regions. *Neuroscience* 2010; 170: 189-199.
- [35] Yagi T and Takeichi M. Cadherin superfamily genes: functions, genomic organization, and neurologic diversity. *Genes Dev* 2000; 14: 1169-1180.
- [36] Sugahara T, Yamashita Y, Shinomi M, Yamano-ha B, Iseki H, Takeda A, Okazaki Y, Hayashizaki Y, Kawai K, Suemizu H and Andoh T. Isolation of a novel mouse gene, mSVS-1/SUSD2, reversing tumorigenic phenotypes of cancer cells in vitro. *Cancer Sci* 2007; 98: 900-908.
- [37] Deng M, Wei L, Zuo X, Tian Y, Xie F, Hu P, Zhu C, Yu F, Meng Y, Wang H, Zhang F, Ma H, Ye R, Cheng H, Du J, Dong W, Zhou S, Wang C, Wang Y, Wang J, Chen X, Sun Z, Zhou N, Jiang Y, Liu X, Li X, Zhang N, Liu N, Guan Y, Han Y, Han Y, Lv X, Fu Y, Yu H, Xi C, Xie D, Zhao Q, Xie P, Wang X, Zhang Z, Shen L, Cui Y, Yin X, Cheng H, Liang B, Zheng X, Lee TM, Chen G, Zhou F, Veldink JH, Robberecht W, Landers JE, Andersen PM, Al-Chalabi A, Shaw C, Liu C, Tang B, Xiao S, Robertson J, Zhang F, van den Berg LH, Sun L, Liu J, Yang S, Ju X, Wang K and Zhang X. Genome-wide association analyses in Han Chinese identify two new susceptibility loci for amyotrophic lateral sclerosis. *Nat Genet* 2013; 45: 697-700.
- [38] Uo T, Veenstra TD and Morrison RS. Histone deacetylase inhibitors prevent p53-dependent and p53-independent bax-mediated neuronal apoptosis through two distinct mechanisms. *J Neurosci* 2009; 29: 2824-2832.
- [39] Takahashi S, Harigae H, Yokoyama H, Kaku M and Sasaki T. Genomic structure and regulation of a novel human gene, Klp1. *Biochim Biophys Acta* 2001; 1522: 207-211.
- [40] Takahashi S, Furuyama K, Kobayashi A, Taketani S, Harigae H, Yamamoto M, Igarashi K, Sasaki T and Hayashi N. Cloning of a coproporphyrinogen oxidase promoter regulatory element binding protein. *Biochem Biophys Res Commun* 2000; 273: 596-602.
- [41] Miki H, Setou M, Kaneshiro K and Hirokawa N. All kinesin superfamily protein, KIF, genes in mouse and human. *Proc Natl Acad Sci U S A* 2001; 98: 7004-7011.
- [42] Vale RD and Fletterick RJ. The design plan of kinesin motors. *Annu Rev Cell Dev Biol* 1997; 13: 745-777.
- [43] Sharp DJ, Rogers GC and Scholey JM. Microtubule motors in mitosis. *Nature* 2000; 407: 41-47.

Molecular mechanism of TGF- β 1-induced differentiation

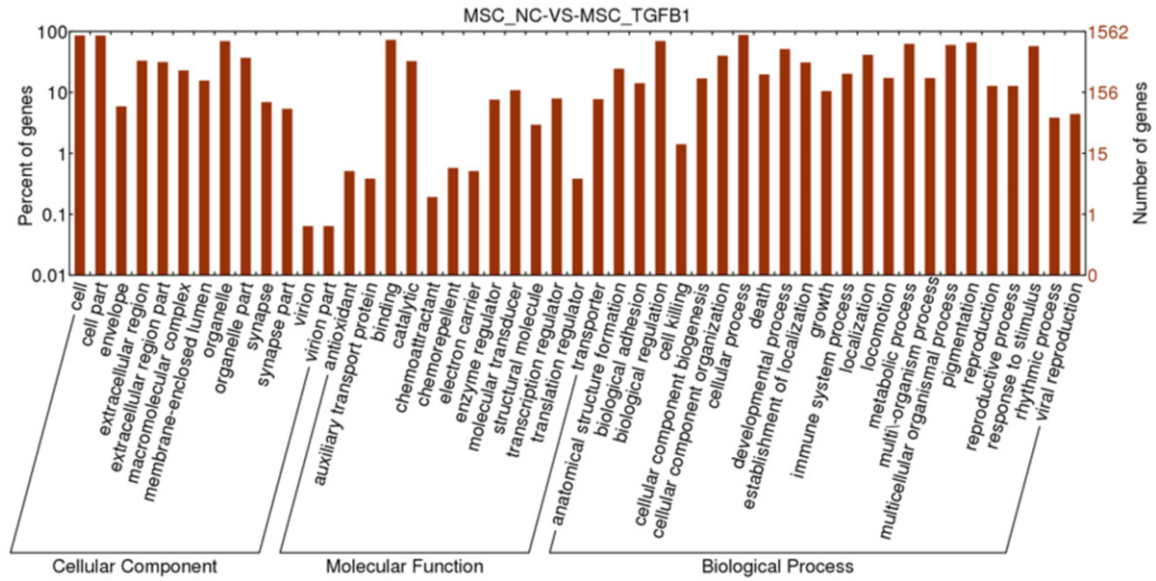


Figure S1. Gene ontology (GO) analysis of differentially expressed genes.

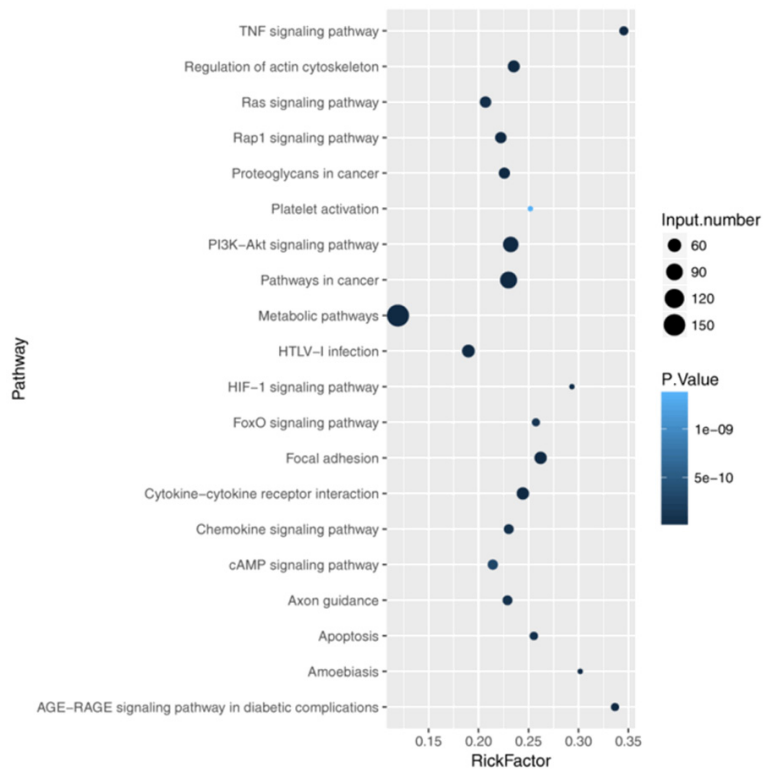


Figure S2. KEGG pathway analysis of differentially expressed genes.